Nucleon-nucleon potential with quark degrees of freedom

M. Beyer*
Institut für Kernphysik, Universität Mainz, D-6500 Mainz, Federal Republic of Germany

H. J. Weber
Department of Physics, University of Virginia, Charlottesville, Virginia 22901
(Received 31 July 1986)

Nucleon-nucleon phase shifts for all partial waves, static properties, and electromagnetic form factors of the deuteron are calculated from an NN potential, which has a mesonic sector with only two adjusted parameters and is supplemented by a phenomenological six-quark core potential with a P-matrix-type parametrization. NN phase shifts constrain the six-quark core radius within $1 \leq b \leq 1.2$ fm. The deuteron's magnetic structure function B agrees with the data only for $b = 1$ fm. The six-quark core probability is about 2.3%.

I. INTRODUCTION

Quantum chromodynamics (QCD) is now widely believed to be the correct theory of the strong interaction.[1] As QCD remains unsolved at low energy and long distances, where color is confined, quark confinement models are usually supplemented by ingredients from perturbative QCD. Examples are the nonrelativistic harmonic-oscillator model (NQM) with a short-ranged color hyperfine interaction between massive ("constituent") quarks[2] and chiral bag models (CBM)[3] with massless ("current") quarks and pion exchange at long distances. In this spirit many old and new problems of nuclear physics have recently been investigated.

Among them the nucleon-nucleon (NN) force remains one of the most challenging and fundamental problems. Conventional NN potentials[4] are based on meson exchange dynamics with adjustable vertex form factors needed for convergence and to include finite size effects. They are successful in fitting the rich data with a dozen or more parameters. However, their ambiguities prevent an understanding of the true nature of NN dynamics, especially at short distances, where quarks are expected to play a more direct role. To the extent that relativistic and quark effects are present in the NN data at longer distances, they are simulated by the parameters of basically nonrelativistic meson exchanges. In the context of electromagnetic interactions such NN potentials are quite successful in predicting photo- and electrodisintegration cross sections from the deuteron, triton, and ^{3}He, when supplemented by pionic exchange (e.g., pair) currents.[5]

Nonetheless it is fair to say that only the one-pion exchange potential (OPEP) is quantitatively confirmed at long distances by the deuteron's D/S ratio of asymptotic wave functions,[6] peripheral NN phase shifts, and pionic exchange current effects.

While meson dynamics has not been derived from QCD, in the limit of infinitely many colors ($N_c \to \infty$) it is known to lead to a meson field theory, in which baryons are topological solitons.[7] This connection is the main motivation for much recent work on Skyrme models,[8] whose results remain in only qualitative agreement with the data, though. The CBM and Skyrme models contain the spontaneous breakdown of chiral invariance expected in the low energy phase of QCD in the form of the nonlinear σ model.[3] The latter also follows from nonlinear spinor models patterned on the Bardeen-Cooper-Schrieffer (BCS) theory of superconductivity starting with the basic work of Nambu and Jona-Lasinio (NJL).[9] In conjunction with the electroweak interactions, such quark models[10] imply also the phenomenology of the vector meson dominance model,[11] thereby supporting the exchange of heavier mesons in one-boson-exchange (OBE) models of NN scattering. Similar conclusions have been independently reached recently from the "hidden" local SU(2) symmetry[12] of the nonlinear σ model, in which the ρ-meson field occurs as a massive Yang-Mills gauge boson in the sense of Ref. 11.

Our NN potential[13] is based on an effective quark interchange mechanism at medium and long distances, which accounts for the quark-antiquark content of the exchanged mesons. It starts from a nonlinear four-quark contact interaction, constrained by QCD symmetries (a NJL model), for a pair of valence quarks at short distances, one from each of the slightly overlapping nucleons at large distances, as is summarized in Sec. II. In Sec. III it is completed by a nonmesonic six-quark model for overlapping nucleons at short distances. The resulting NN phase shifts, low energy parameters, and deuteron properties are shown in Sec. IV and V.

II. NN POTENTIAL AT LONG DISTANCES

The mesonic NN potential is constructed to depend on the underlying quark model directly. This is in contrast to conventional NN potentials, where finite-size vertex form factors and the corresponding meson-nucleon coupling constants are adjusted independently.

To take color confinement into account, one can place massive constituent quarks in a nonrelativistic harmonic oscillator well (NQM), or massless ("current") quarks in a spherical cavity in the MIT bag model.[2] The color mag-

netic hyperfine interaction (chf) suggested by gluon exchange at short interquark distances then provides the observed spin splittings in the N-Δ, Σ-Λ, and, to some extent, the π-ρ systems.

Relativistic corrections to the NQM have been included in a model abbreviated as CQM, which is used in the following.[13] With pion-exchange corrections at long distances the CQM has been successfully applied to baryon magnetic moments,[14] the electromagnetic and axial form factors of the nucleon,[15] semileptonic hyperon decays[16] and the pionic pair and exchange currents.[17]

However, the phenomenological scalar confinement potentials of quark models are independent of spin and thereby violate chiral invariance. To restore the global γ_5 symmetry of QCD in CBM's an elementary pion field is introduced to chirally rotate the quark's helicity, when the quark reflects from the nucleon's surface. The resulting pion-quark coupling corresponds to a nonlinear σ model.[3]

Although the constituent quark size of about $\frac{1}{3}$ fm has been estimated,[18] we treat quarks as pointlike Dirac particles with a mass $m_u=m_d=m_Q\sim m_N/3$ independent of momentum. In essence, we assume that the $q\bar{q}$ and gluon condensates play a role also inside nucleons; this is consistent with QCD sum rule results[19] and removes the sharp nucleon surface of CBM's.

Mesons are then represented as mean fields Φ_α with their physical mass m_α and may propagate inside nucleons. The quark-interchange model of the quark-one-boson-exchange potential has been described in detail elsewhere.[13] It is given by

$$V_{\text{Q-OBE}}(q^2)=G^2\sum_\alpha O'_\alpha(q^2-m_\alpha^2)^{-1}O_\alpha\ , \tag{1}$$

where $q=p'_1-p_1=p_2-p'_2$ is the (nucleon) momentum transfer and G is determined from the pion-nucleon coupling constant (cf. Table I)

$$g^2_{\pi NN}/4\pi\approx 14.0,\quad g_{\pi NN}=\tfrac{5}{3}GN_0^2 2m_N/3m_Q\ . \tag{2}$$

The scalar-isoscalar σ-meson ($O_\alpha=1$) and pion ($O_\alpha=i\gamma_5\tau$) have the same quark coupling constant, as implied by the underlying chiral invariant NJL nonlinear quark-spinor model.[10,13] As expected from the σ model, the chiral symmetry is broken by the introduction of meson masses in the free propagators in (1).

TABLE I. Meson-nucleon coupling constants at $\mathbf{q}^2=0=q^0$ from the CQM.

Scalar:	$g^2_{\epsilon NN}=9G^2N_0^4(1-\alpha^2/4m_Q^2)^2$
	$g^2_{\delta NN}=G^2N_0^4(1-\alpha^2/4m_Q^2)^2$
Pseudoscalar:	$g^2_{\eta NN}=G^2N_0^4 4m_N^2/9m_Q^2$
	$g^2_{\pi NN}=\frac{25}{9}G^2N_0^4 4m_N^2/9m_Q^2$
Vector:	$g^2_{\omega NN}=9G^2/2$
	$f_{\omega NN}=GN_0^2/\sqrt{2}\,(2m_N/3m_Q-3N_0^{-2})$
	$g^2_{\rho NN}=G^2/2$
	$f_{\rho NN}=GN_0^2/\sqrt{2}\,(10m_N/9m_Q-N_0^{-2})$
Axial-vector:	$g^2_{ANN}=\frac{25}{18}G^2N_0^4(1-\alpha^2/12m_Q^2)^2$
	$f_{ANN}=-\frac{5}{3}GN_0^2/\sqrt{2}\,4m_N^2/18m_Q^2$
	$g^2_{DNN}=G^2N_0^4/2(1-\alpha^2/12m_Q^2)^2$
	$f_{DNN}=-GN_0^2/\sqrt{2}\,4m_N^2/18m_Q^2$

To construct the NN potential that follows from (1), it has to be evaluated between three-quark wave functions

$$\Psi_N=\Phi(\mathbf{r}_1,\mathbf{r}_2,\mathbf{r}_3)\chi_{SF}C\ , \tag{3}$$

where S,F stand for spin and flavor quantum numbers, and C for the antisymmetric color wave function. To include relativistic corrections to lowest order for the interacting quark, the quark wave function is defined as

$$\Phi(\mathbf{r}_1,\mathbf{r}_2,\mathbf{r}_3)=N_0\begin{pmatrix}1\\ -i\boldsymbol{\sigma}\cdot\boldsymbol{\nabla}/2m_Q\end{pmatrix}\prod_{j=1}^{3}g(\mathbf{r}_j) \tag{4}$$

with

$$g(\mathbf{r}_j)=(\alpha/\sqrt{\pi})\exp[-\alpha^2(\mathbf{r}_j^2-\mathbf{R}^2/3)/2]\ ,\qquad N_0^{-2}=1+\alpha^2/4m_Q^2 \tag{5}$$

and the usual relative Lovelace coordinates $\boldsymbol{\rho},\boldsymbol{\lambda}$, viz.,

$$\boldsymbol{\rho}=(\mathbf{r}_1-\mathbf{r}_2)/\sqrt{2}\ ,\quad \boldsymbol{\lambda}=(\mathbf{r}_1+\mathbf{r}_2-2\mathbf{r}_3)/\sqrt{6}\ ,\quad \mathbf{R}=(\mathbf{r}_1+\mathbf{r}_2+\mathbf{r}_3)/\sqrt{3}\ . \tag{6}$$

TABLE II. Comparison of numerical values of meson-nucleon coupling constants from various models.

Meson (J^P,T)	Mass (GeV)	MIT bag	Linear confinement	CQM $m_Q=0.33$ GeV $b=1$ fm	CQM $m_Q=0.33$ GeV $b=1.2$ fm	CQM $m_Q=0.22$ GeV	Bonn
$\epsilon(0^+,0)$	1.2	3.89	4.53	6.79	7.09	1.10	
$\delta(0^+,1)$	0.96	0.44	0.5	0.75	0.79	0.12	1.69
$\eta(0^-,0)$	0.5485	4.87	5.32	4.83	5.04	5.18	
$\pi(0^-,1)$	0.1385	13.4	14.8	13.4	14.0	14.4	14.08
$\omega(1^-,0)$	0.7823	6.0 (−0.4)	3.78 (−0.5)	9.44 (−0.49)	9.85 (−0.49)	7.04 (−0.39)	10.6 (−)
$\rho(1^-,1)$	0.763	0.67 (2.2)	0.42 (3.2)	1.05 (1.53)	1.10 (1.53)	0.78 (2.03)	0.41 (6.1)
$D(1^+,0)$	1.285	0.6 (−1.5)	0.22	0.56	0.59	0.21	
$A_1(1^+,1)$	1.1	1.1	0.6	1.57	1.64	0.59	
$\sigma'(0^+,0)$	0.6						5.33

The radial three-quark nucleon ground state wave function from (5) is the solution of the Schrödinger equation in a harmonic oscillator confinement potential

$$V=\frac{\kappa}{2}\sum_{i<j=1}^{3}(\mathbf{r}_i-\mathbf{r}_j)^2=\frac{3\kappa}{2}(\boldsymbol{\rho}^2+\boldsymbol{\lambda}^2)\ , \tag{7}$$

with $\alpha^4=3\kappa m_Q$, and has the form

$$\prod_{j=1}^{3} g(\mathbf{r}_j)=(\alpha/\sqrt{\pi})^3\exp[-\alpha^2(\boldsymbol{\rho}^2+\boldsymbol{\lambda}^2)/2]\ . \tag{8}$$

In momentum space the OBE potential takes the form

$$\begin{aligned}V_{\text{Q-OBE}}(q^2)=&[g^2_{\epsilon\text{NN}}(q^2-m_\epsilon^2)^{-1}+g^2_{\delta\text{NN}}\boldsymbol{\tau}'\cdot\boldsymbol{\tau}(q^2-m_\delta^{-1})]1'\cdot 1-[g^2_{\eta\text{NN}}(q^2-m_\eta^2)^{-1}+g^2_{\pi\text{NN}}\boldsymbol{\tau}'\cdot\boldsymbol{\tau}(q^2-m_\pi^2)^{-1}]\gamma_5'\cdot\gamma_5\\
&-(g_{\omega\text{NN}}\gamma'_\mu+if_{\omega\text{NN}}\sigma'_{\mu\nu}q^\nu/2m_\text{N})(q^2-m_\omega^2)^{-1}(g_{\omega\text{NN}}\gamma^\mu-if_{\omega\text{NN}}\sigma^{\mu\nu}q_\nu/2m_\text{N})\\
&-(g_{\rho\text{NN}}\gamma'_\mu+if_{\rho\text{NN}}\sigma'_{\mu\nu}q^\nu/2m_\text{N})\boldsymbol{\tau}'\cdot\boldsymbol{\tau}(q^2-m_\rho^2)^{-1}(g_{\rho\text{NN}}\gamma^\mu-if_{\rho\text{NN}}\sigma^{\mu\nu}q_\nu/2m_\text{N})\\
&-(g_{D\text{NN}}\gamma'_\mu\gamma'_5+f_{D\text{NN}}\gamma'_5q_\mu/m_\text{N})(q^2-m_D^2)^{-1}(g_{D\text{NN}}\gamma^\mu\gamma_5-f_{D\text{NN}}\gamma_5q^\mu/m_\text{N})\\
&-(g_{A\text{NN}}\gamma'_\mu\gamma'_5+f_{A\text{NN}}\gamma'_5q_\mu/m_\text{N})\cdot\boldsymbol{\tau}'\cdot\boldsymbol{\tau}(q^2-m_A^2)^{-1}(g_{A\text{NN}}\gamma^\mu\gamma_5-f_{A\text{NN}}\gamma_5q^\mu/m_\text{N})\ ,\end{aligned} \tag{9}$$

with the CQM coupling constants shown in Table I. Numerical values from different quark models are shown in Table II. The corresponding potential version in coordinate space, which we have used to solve the Schrödinger equation, is given as

$$\begin{aligned}V_{\text{Q-OBE}}(r)=&-g^2_{\epsilon\text{NN}}/4\pi[I_{00}(m_\epsilon r)-I_{02}(m_\epsilon r)/4m_\text{N}^2-\mathbf{L}\cdot\mathbf{S}I_{10}(m_\epsilon r)/2m_\text{N}^2]\\
&-g^2_{\delta\text{NN}}/4\pi[I_{00}(m_\delta r)-I_{02}(m_\delta r)/4m_\text{N}^2-\mathbf{L}\cdot\mathbf{S}I_{10}(m_\delta r)/2m_\text{N}^2]\boldsymbol{\tau}'\cdot\boldsymbol{\tau}\\
&+g^2_{\eta\text{NN}}/4\pi[I_{02}(m_\eta r)\boldsymbol{\sigma}'\cdot\boldsymbol{\sigma}+\hat{S}I_{20}(m_\eta r)]/12m_\text{N}^2\\
&+g^2_{\pi\text{NN}}/4\pi[m_\pi^2I_{00}(m_\pi r)\boldsymbol{\sigma}'\cdot\boldsymbol{\sigma}+\hat{S}I_{20}(m_\pi r)]\boldsymbol{\tau}'\cdot\boldsymbol{\tau}/12m_\text{N}^2\\
&+g^2_{\omega\text{NN}}/4\pi\{I_{00}(m_\omega r)+(1+\kappa_\omega)I_{02}(m_\omega r)/2m_\text{N}^2+(3+4\kappa_\omega)\mathbf{L}\cdot\mathbf{S}I_{10}(m_\omega r)/2m_\text{N}^2\\
&\qquad+(1+\kappa_\omega)^2[2\boldsymbol{\sigma}'\cdot\boldsymbol{\sigma}I_{02}(m_\omega r)]-\hat{S}I_{20}(m_\omega r)]/12m_\text{N}^2\}\\
&+g^2_{\rho\text{NN}}/4\pi\{I_{00}(m_\rho r)+(1+\kappa_\rho)I_{02}(m_\rho r)/2m_\text{N}^2+(3+4\kappa_\rho)\mathbf{L}\cdot\mathbf{S}I_{10}(m_\rho r)/2m_\text{N}^2\\
&\qquad+(1+\kappa_\rho)^2[2\boldsymbol{\sigma}'\cdot\boldsymbol{\sigma}I_{02}(m_\rho r)-\hat{S}I_{20}(m_\rho r)]/12m_N^2\}\boldsymbol{\tau}'\cdot\boldsymbol{\tau}\\
&+g^2_{D\text{NN}}/4\pi I_{00}(m_D r)\boldsymbol{\sigma}'\cdot\boldsymbol{\sigma}+g^2_{A\text{NN}}/4\pi I_{00}(m_A r)\boldsymbol{\sigma}'\cdot\boldsymbol{\sigma}\boldsymbol{\tau}'\cdot\boldsymbol{\tau}\ ,\end{aligned} \tag{10}$$

$$V_{\text{Q-TPE}}(r)=-(g^2_{\sigma_0\text{NN}}+g^2_{\sigma_1\text{NN}}\boldsymbol{\tau}'\cdot\boldsymbol{\tau})I_{00}(m_\sigma r)/4\pi\ , \tag{11}$$

with $\kappa=g/f$, and

$$I_{00}(x)=m\exp(x_0^2)/2x[e^{-x}\text{erfc}(x_0-x/2x_0)-(\text{“}x\leftrightarrow -x\text{”})]\ , \tag{12}$$

$$x=mr,\quad x_0=m/\alpha\sqrt{3},\quad \text{erfc}(z)=1-\text{erf}(z),\quad \text{erf}(z)=2/\sqrt{\pi}\int_0^z\exp(-t^2)dt\ , \tag{13}$$

$$I_{\rho\lambda}(mr)=r^\rho(d/r\,dr)^\rho\nabla_r^\lambda I_{00}(mr)\ . \tag{14}$$

Explicitly,

$$I_{10}(x)=-m^2\exp(x_0^2)/2x^2[(1+x)e^{-x}\text{erfc}(x_0-x/2x_0)+(\text{“}x\leftrightarrow -x\text{”})]+m^2\exp(-x^2/4x_0^2)/xx_0\sqrt{\pi}\ , \tag{15}$$

$$I_{02}(x)=m^2I_{00}(x)-m^3\exp(-x^2/4x_0^2)/2x_0^3\sqrt{\pi}\ , \tag{16}$$

$$\begin{aligned}I_{20}(x)=&m^3\exp(x_0^2)/2x^3[(3+3x+x^2)e^{-x}\text{erfc}(x_0-x/2x_0)-(\text{“}x\leftrightarrow -x\text{”})]\\
&-3m^3(1+x^2/6x_0^2)\exp(-x^2/4x_0^2)/x^2x_0\sqrt{\pi}\ .\end{aligned} \tag{17}$$

Moreover, $\mathbf{L}=\mathbf{r}\times\mathbf{p}$ is the orbital angular momentum operator with reduced matrix element $\langle L||L||L\rangle=\sqrt{L(L+1)}$, $\mathbf{S}=(\boldsymbol{\sigma}'+\boldsymbol{\sigma})/2$ is the spin operator, and the tensor operator

$$\hat{S}=3[r^{[2]}\times[\sigma'^{[1]}\times\sigma^{[1]}]^{[2]}]^{[0]}$$

in a spherical basis with

$$[a^{[n]}\times b^{[n]}]^{[0]}=\sum C^{n\,n\,0}_{m\,-m\,0}\,a^n_m b^n_{-m}\ . \tag{18}$$

III. NN POTENTIAL AT SHORT DISTANCES

As a consequence of the strong damping provided by the bound quark wave functions, the meson exchange potentials become generally negligible[13] inside distances of about 1 fm, in contrast to conventional NN potentials,[4] which depend sensitively on adjusted short-range cutoff parameters. This feature allows us to introduce a phenomenological nonmesonic six-quark core potential at

short distances. Its parametrization in coordinate space is patterned after the P-matrix approach of the compound bag model.[20] Since the NN continuum is described by meson exchange potentials, the remaining six-quark spectrum is discrete with energies E_n and states φ_n. A motivation for this approach has been given in Ref. 20. The optical potential is defined as

$$V_h(\mathbf{r},\mathbf{r}';E)=\sum_n \langle \mathbf{r} \mid V_{hn} \mid \varphi_n \rangle \langle \varphi_n \mid V_{nh} \mid \mathbf{r}' \rangle /(E-E_n) \ . \tag{19}$$

The transition potential V_{nh} from the six-quark core to the hadronic NN channels consists of a surface term V_t with the pole structure of the P-matrix and a volume term from

$$\begin{aligned} &\langle \varphi_h \mid \varphi_n \rangle \neq 0 \ , \\ &\langle \varphi_h \mid V_{hn} \mid \varphi_n \rangle = \langle \varphi_h \mid V_t \mid \varphi_n \rangle + (E_n - E)\langle \varphi_h \mid \varphi_n \rangle \ . \end{aligned} \tag{20}$$

Integrating on the right hand side with respect to the internal motion we get

$$\begin{aligned} &\langle \varphi_h \mid \varphi_n \rangle \propto \chi_{ST}(\mathbf{r}) y_n(\mathbf{r}) \\ &\langle \varphi_h \mid V_t \mid \varphi_n \rangle \propto \chi_{ST}(\mathbf{r}) V_t(\mathbf{r}) y_n(\mathbf{r}) \ , \end{aligned} \tag{21}$$

where $\chi_{ST}(\mathbf{r})$ and $y_n(\mathbf{r})$ are the wave functions of relative distance of three-quark clusters in the hadronic and six-quark channel, respectively. Choosing $V_t(\mathbf{r})=V_t^0\delta(r-b)$, we arrive at our potential parametrization

$$\begin{aligned} V_h(r,E)=&c_0^2\delta(r-b)/(E-E_0) \\ &+[(E-E_0)c_2^2+c_1]\Theta(b-r) \ , \end{aligned} \tag{22}$$

or equivalently

$$\begin{aligned} V_h(r,E)=&c_0^2\delta(r-b)/(E-E_0) \\ &+(y_0E_0+y_1E)\Theta(b-r) \ . \end{aligned} \tag{22'}$$

The parameters c_0, c_2 are related to the six-quark model as

$$\begin{aligned} &c_0 \propto V_t^0 \eta_l(b) \ , \\ &c_2 \propto \int_0^\infty u_l(r)\eta_l(r)dr \ , \end{aligned} \tag{23}$$

where $\eta_l(r)$ and $u_l(r)$ are the appropriate radial wave functions of the partial wave decomposition of $y_n(r)$ and $\chi_{ST}(r)$, respectively. The lowest six-quark energy eigenvalue E_0 in (22) is calculable if a full six-quark Hamiltonian is given. The parameter b is a measure of the extent of the six quark core region.

For lack of an appropriate six quark Hamiltonian both parameters are chosen to have certain values (cf. Sec. IV). At this stage V_t is assumed to be a central potential only, but for further numerical calculations we also allow V_t to contain tensor and spin orbit terms.

The linear energy dependence of the short range NN potential as parametrized already by the Paris potential is, at least qualitatively, explained by taking into account the quark structure of the nucleon.

The two parts of the optical potential in (22) are displayed in Figs. 1 and 2 at a six quark core radius b

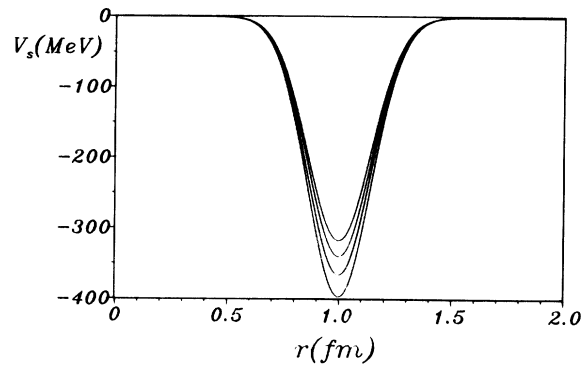

FIG. 1. Surface part of the optical potential for the $^1S_0$ channel and $b=1$ fm at lab energies $E_{\rm lab}=0$, 100, 200, and 300 MeV.

$=1$ fm for the $^1S_0$ channel. The surface term becomes more attractive with higher energies, whereas the volume term is more repulsive at higher scattering energy.

For numerical convenience the δ distribution and the step function Θ are smeared out according to

$$\begin{aligned} &\delta(r-b)\rightarrow \exp[-(r-b)^2/\epsilon^2]/\epsilon\sqrt{\pi} \ , \\ &\Theta(b-r)\rightarrow [1+(r/b)^{20}]^{-1} \ , \end{aligned} \tag{24}$$

where $\epsilon=0.2$ and 0.1 fm for $b=1$ and 1.2 fm, respectively.

IV. NN PHASE SHIFTS

We have used our potential, which is more consistent with the internal quark structure of the nucleon and its excited states than conventional NN potentials, to extract various parameters of the six-quark core. In particular, we have analyzed its dependence on the radius b of the six-quark core region. We find that values $b<1$ fm and $b>1.2$ fm disagree with the NN phase shift data, so we present our results only for the values $b=1$ and 1.2 fm. Since the potential depends only weakly on the lowest six-quark core level E_0, we have chosen $E_0=750$ MeV, which corresponds to that of the P-matrix analysis[21] for $b=1.2$ fm.[22]

For $m_\sigma=495$ MeV/c^2 of Ref. 23 we show in Table III our adjusted effective σ-meson exchange parameters

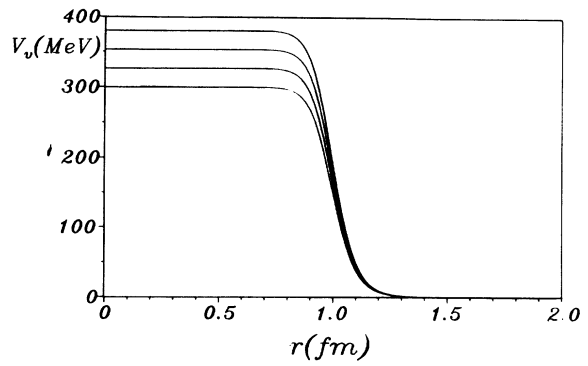

FIG. 2. Volume part of the optical potential for the same parameters as in Fig. 1.

TABLE III. Pion-quark and adjusted σ-meson-nucleon coupling constants for six-quark core radius $b=1$ and 1.2 fm.

	$b=1$ fm	$b=1.2$ fm
$G^2/4\pi$	2.0973	2.1893
$g^2_{\sigma_0 NN}/4\pi$	3.3192	3.0273
$g^2_{\sigma_1 NN}/4\pi$	0.7608	0.6727

TABLE IV. Adjusted six-quark core parameter y_0 of Eq. (22') for P and D waves and six-quark core radius $b=1$ and 1.2 fm.

	$^1P_1$	$^3P_0$	$^3P_1$	$^3P_2$	$^1D_2$	$^3D_3$
y_0 ($b=1$ fm)	0.4	0.6	0.45	−0.03	−0.22	−0.4
y_0 ($b=1.2$ fm)	0.15	0.17	0.13	−0.05	−0.11	−0.15

($g_{\sigma_0}, g_{\sigma_1}$), which reproduce the phase shifts of partial waves with $L>2$ that depend only on the OPE and TPE. Heavier meson exchanges are suppressed by the soft vertex form factors from the bound quark wave functions and the angular momentum barrier. In these peripheral partial waves it is reasonable to neglect six-quark core contributions.

In Figs. 3(a)—3(g) we show our phase shift for $L>2$ compared with recent energy dependent (short dashed lines) and single energy analyses (dots) given by Arndt *et al.*[24] There is no substantial deviation from the data. The difference between the phase shifts for $b=1$ and 1.2 fm is mainly due to the cutoff at b of the meson potentials and is not a six-quark effect. This requires the small renormalization of G^2 and $g^2_{\sigma_i}$ shown in Table III.

However, there is some contribution of the six-quark core in some D and all P waves. Since it is not possible to extract all parameters of the core potential from these partial waves, we have assumed an energy independent mean value for the core potential, viz., $y_1=c_0=0$ in (22) and (22'), which is treated as a volume term. Thus, for each partial wave in P and some D waves we have one parameter to adjust to the energy dependence of the phase shifts. Table IV shows the relevant parameters for partial waves with a core contribution. We want to emphasize that our short-range potential need not be repulsive (which is the case of some potentials with a large ωNN coupling).

Figures 4(a)—4(h) show the P and D phase shifts. Except for the $^1P_1$ phase shift, where $\Delta(1232)$ degrees of freedom may be important, all partial-wave phase shifts agree with the experimental values. At higher energies the $b=1.2$ fm case gives too much attraction in the $^3P_1$ phase shift.

Most recent discussions emphasizing the short range part of the NN potential concentrate on $L=0$ partial waves, which have no angular momentum barrier. However, we have seen that for P and D waves there is still some influence of the six-quark core. The S phase shifts are sensitive enough to separate the potential coming from the P-matrix pole from that originating from the overlap integrals. Its parameters are displayed in Table V.

In the $^3S_1$-$^3D_1$ channel we need a tensor force in the transition potential V_t,

$$V_T(r,E)=c_T^2\delta(r-b)/(E-E_0)\ , \tag{25}$$

where c_T is adjusted to the quadrupole moment of the deuteron, which is about 10% too low for $c_T=0$. This V_T is purely attractive and gives the correct energy dependence of the mixing angle $\bar{\epsilon}_1$ as well.

In Table VI we compare the pole part of the optical potential with the parameters of a P-matrix analysis of Bakker *et al.*[21] Our residues $\tau_0=4m_N c_0^2$ are somewhat higher.

In Figs. 5(a) and 5(b) we have displayed the phase shifts δ_0, $\bar{\delta}_0$ of the $^1S_0$, $^3S_1$-$^3D_1$ partial waves. The reasonable agreement of both cases $b=1$ and 1.2 fm with the experimental analyses is not surprising, as the phenomenological six-quark core model forces us to admit three additional parameters for each S wave. Two of these parameters are largely determined by the low-energy dependence of the phase shifts and the static deuteron properties. The scattering lengths a_s, a_t and effective ranges r_s, r_t in Table VII determine c_0^2 and y_0. Only one parameter in each partial wave is adjusted to the energy dependence of the phase shift.

The model parametrization of (22),(22') does not provide reasonable values for the effective ranges for $b>1.2$ fm, whereas for $b<1$ fm the correct energy dependence of S-wave phase shifts cannot be obtained. These constraints on the six-quark core size will be narrowed further by the magnetic form factor of the deuteron in Sec. VI.

Compared to our complete potential analysis below the pion production threshold, the ITEP group[20] has considered only a few low partial waves, but fitted the corresponding phase shifts to higher energies. The extracted $b\approx 1.5$ fm is larger than our $b=1$ fm. In another P-matrix analysis[25] of several low NN partial-wave phase shifts the P-matrix pole predictions of quark bag models are compared to each other and NN data. The extracted $b=1.05$ fm is close to ours, but the pole positions lie far above the energy regime, where these quark models and the nonrelativistic analysis apply. Moreover, the NQM and the CQM extensions we use have not been considered.

A hybrid quark model[26] uses the wave functions from a conventional NN potential at internucleon distances larger than some adjustable cutoff radius $r_0=b$, where matching conditions to inner multiquark configurations are imposed. Although the proper phase shifts are maintained

TABLE V. Adjusted six-quark core parameters y_0, y_1, c_0^2/E_0, and c_T^2/E_0 of Eqs. (22), (22'), and (25) for the S waves and six-quark core radius $b=1$ and 1.2 fm.

		y_0	y_1	c_0^2/E_0	c_T^2/E_0
$b=1$ fm	$^1S_0$	0.4	0.533	0.57	
	$^3S_1$	0.4	0.733	0.55	0.3
$b=1.2$ fm	$^1S_0$	0.32	0	0.5071	
	$^3S_1$	0.2	0	0.3691	0.19

TABLE VI. Comparison of the six-quark pole energy and residue of the optical potential with core radius $b=1.2$ fm with various potentials of Ref. 21.

		Our model	No potential	OPEP	RSC	Paris
$^1S_0$	$\sqrt{s_0}$ (GeV)	2.37	2.330	2.335	2.349	2.342
	τ_0 (GeV^3)	1.43	1.066	1.085	1.131	1.057
$^3S_1$	$\sqrt{s_0}$ (GeV)	2.37	2.206	2.235	2.236	2.236
	τ_0 (GeV^3)	1.04	0.63	0.66	0.67	0.65

TABLE VII. Scattering lengths a_s, a_t and effective ranges r_s, r_t for our NN potential with six-quark core radius $b=1$ and 1.2 fm.

	$b=1$ fm	$b=1.2$ fm	Experiments
a_t (fm)	5.400	5.410	5.423(5)
a_s (fm)	−23.715	−23.715	−23.715(15)
r_t (fm)	1.722	1.807	1.748(14)
r_s (fm)	2.72	2.85	2.73(6)

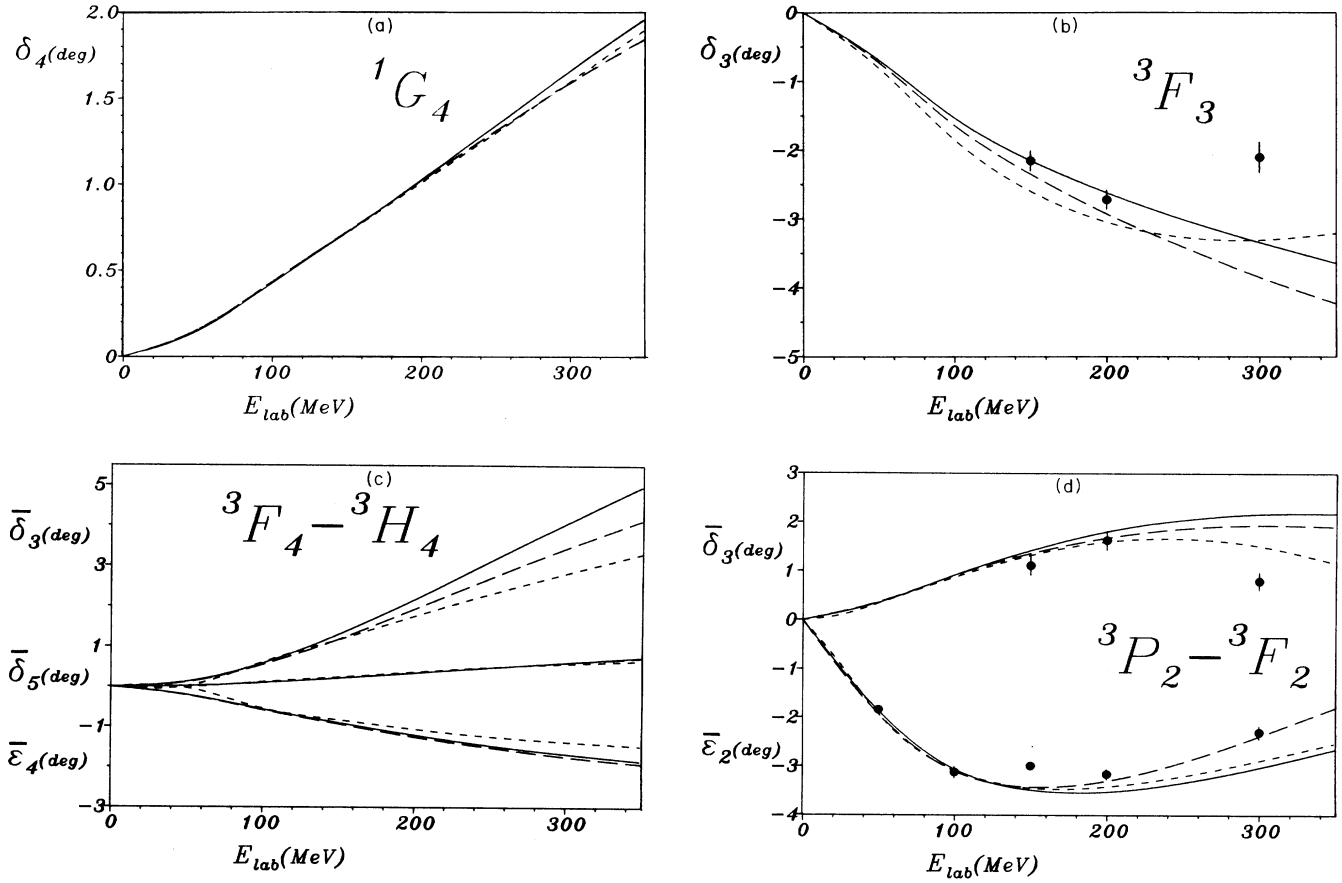

FIG. 3. Phase shifts and mixing angles for $L>2$. Solid line denotes our model with $b=1$ fm; long dashed line, our model with $b=1.2$ fm; dashed line, energy dependent analysis of Ref. 24; dots with error bars, energy independent analysis of Ref. 24.

this way, a corresponding cutoff in the underlying NN potential would require refitting the scattering lengths, effective ranges, and deuteron observables, which is not done. Nonetheless, estimates of six-quark admixture probabilities and their size can be extracted.[27] Although their $b=1$ fm from deuteron electrodisintegration data agrees with our value, it is not as firmly pinned down as ours by elastic electron deuteron scattering (in Sec. V), because of difficulties arising at short range from inconsistent form factors from the inner quark model and the external NN potential.

TABLE VIII. Static deuteron observables for our NN potentials with six-quark core radius $b=1$ and 1.2 fm.

	$b=1$ fm	$b=1.2$ fm	Experiments
E_B (MeV)	2.224 62	2.224 62	2.224 62(6)
Q_D (fm^2)	0.276	0.286	0.2860(15)
D/S (%)	2.58	2.63	2.56(4)
P_D (%)	5.7	5.3	5(3)
P_{6q} (%)	2.3	4.4	
$(\langle r^2\rangle)^{1/2}$ (fm)	1.96	1.99	1.9635(45)

V. DEUTERON PROPERTIES

In Table VIII we give the deuteron results in comparison with the experimental data.

A six-quark core probability[28]

$$P_{6q}=1-\int_b^\infty [u^2(r)+w^2(r)]dr \tag{26}$$

is shown in Table VIII as a guideline for six-quark core effects in our model.

The D/S ratio of asymptotic deuteron wave functions is well known to depend predominantly on the OPEP. The agreement shown in Table VIII with a soft πNN quark-model form factor compares favorably with that of the Paris potential without explicit πNN-form factor.

In Figs. 6(a) and (b) we show our deuteron S and D wave functions in comparison with those of the Reid and Paris potentials. Significant differences occur only for momentum transfer $q>4$ fm despite the softer vertex form factors from the constituent quark model. The differential cross section for elastic electron scattering on deuteron is given by

$$\frac{d\sigma}{d\Omega}=\left[\frac{d\sigma}{d\Omega}\right]_{\text{Mott}}[A(q^2)+B(q^2)\tan^2(\theta/2)]\ , \tag{27}$$

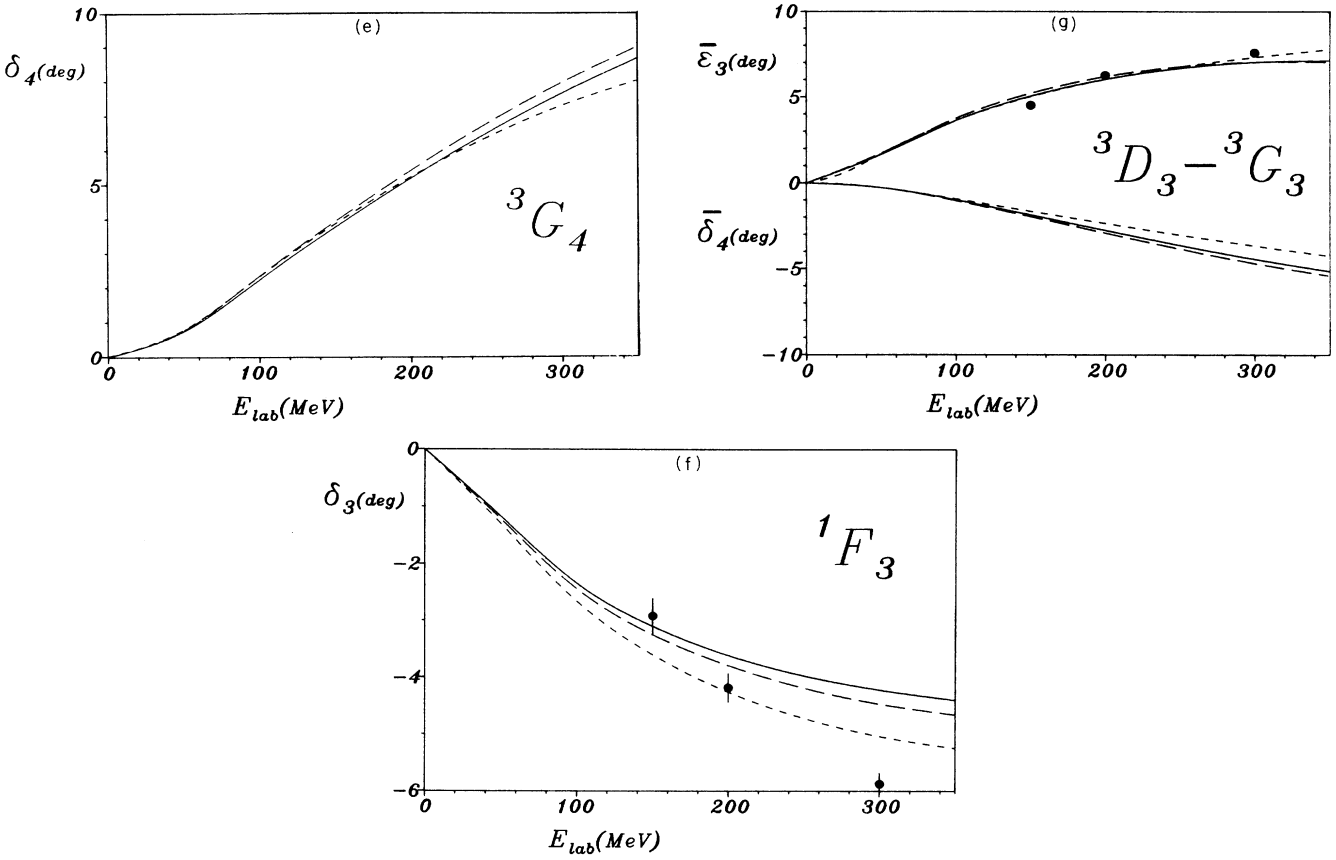

FIG. 3. (*Continued*).

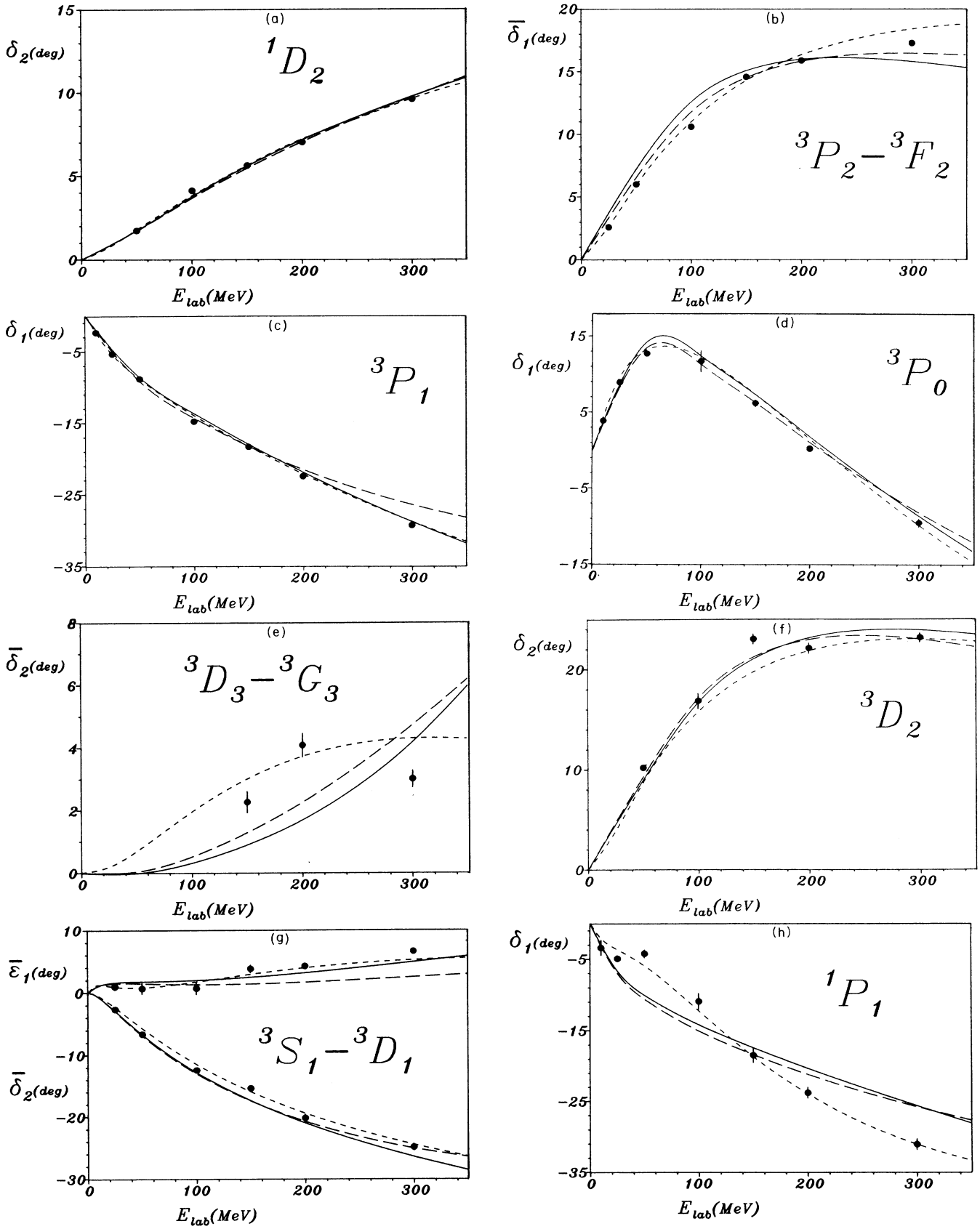

FIG. 4. Phase shifts and mixing angles for P and D waves. For curves, see caption of Fig. 3.

where $(d\sigma/d\Omega)_{\text{Mott}}$ is the Mott cross section, $A(q^2)$ and $B(q^2)$ are elastic form factors depending on the virtual photon momentum q^2, and θ is the electron scattering angle in the laboratory frame. The structure function $A(q^2)$ shown in Fig. 7(a) agrees with the data and those from other potentials, but is not sensitive enough to distinguish between the fine structure in the short range part of the different potentials. However, we found significant deviations between our models with $b=1$ and $b=1.2$ fm in the magnetic form factor $B(q^2)$. This form factor is quite sensitive to the short range parametrization. For example, the position of the node in the magnetic form factor depends on the size of the six-quark core and is shifted to higher values of q^2 for lower b. Thus, as implied by Fig. 7(b), $B(q^2)$ does not agree with the data unless $b \leq 1$ fm. In our form factor results we have also included effects coming from meson exchange currents (MEC's) via the dominant pionic $q\bar{q}$ pair current as given in Ref. 29. Since the deuteron is isoscalar, there is no strong model dependence if one uses a π-N$\bar{\text{N}}$ pair current with a monopole form factor of mass $\Lambda \sim 500$ MeV/c^2.

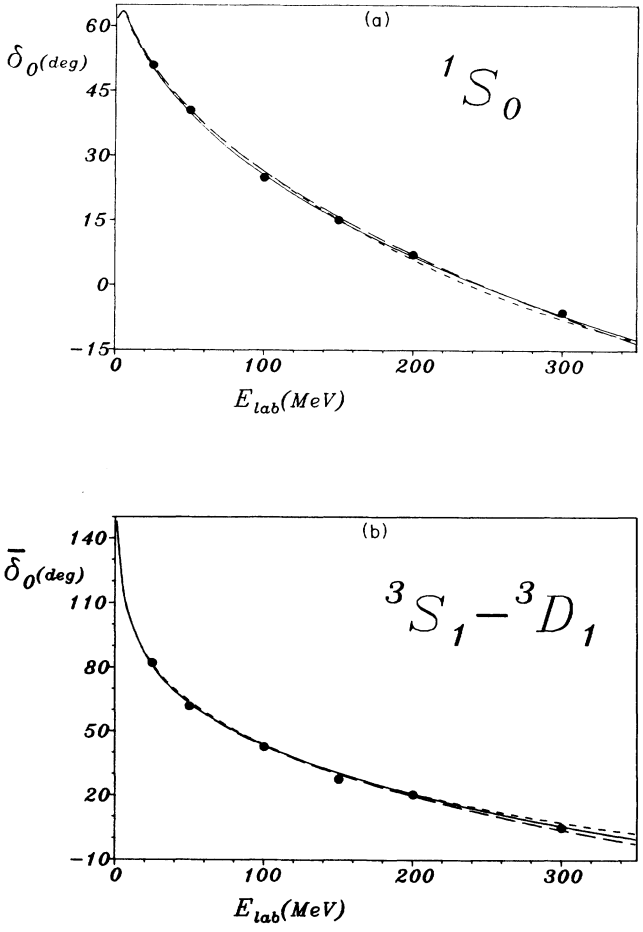

FIG. 5. S wave phase shifts. For curves, see caption of Fig. 3.

The deuteron tensor polarization

$$T(q^2)=4\eta\sqrt{2/3}\frac{G_C(q^2)G_Q(q^2)+\frac{1}{3}\eta G_Q^2(q^2)}{G_C^2(q^2)+\frac{8}{9}\eta^2 G_Q^2(q^2)}\,,$$

$$\eta=-q^2/4m_d^2 \quad (28)$$

is known to be sensitive to the admixture of a six-quark core.[30] Our prediction in Fig. 8, which includes the MEC, is comparable to that of the Paris potential because our NN model does not include a direct short-range six-quark

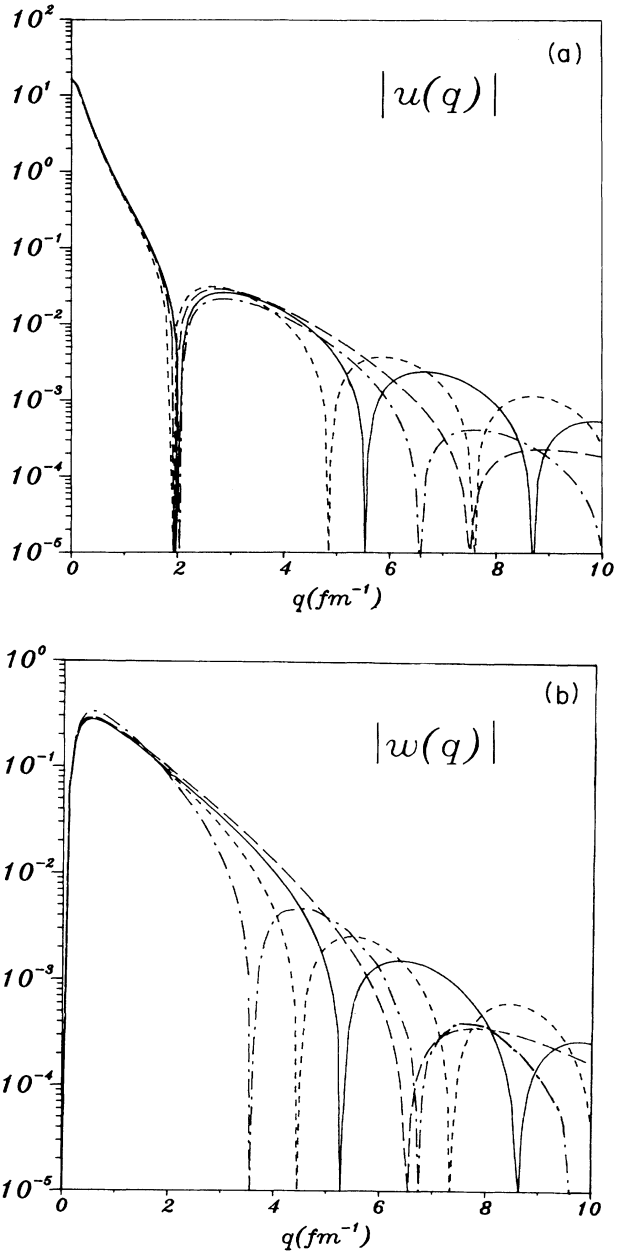

FIG. 6. Deuteron S-wave function u and D-wave function w in momentum space in fm$^{3/2}$. Solid line denotes our model with $b=1$ fm; dashed line, our model with $b=1.2$ fm; long dashed line, RSC potential; long dashed-dotted line, Paris potential.

potential V_q besides the transition potential V_{hq}. We have also included a direct six-quark contribution

$$G_C \to G_C + P_{6q}(1-q^2/4E_0^2)^{-5} \times \exp[q^2b^2(1-15/2b^2E_0^2)/6(1-q^2/4E_0^2)] \tag{29}$$

that is shown in Fig. 8. The six-quark interference term has been shown to be small.[30] The dramatic six-quark core effect of Ref. 30, which is already degraded by the pair charge, appears only for unusually small six-quark core radius $b \sim \frac{3}{4}$ fm and large $P_{6q} \sim 7\%$, whereas our six-quark core parameters give only small effects. The remaining polarization observables (including MEC corrections where applicable) are shown in Figs. 9(a)—9(b) and agree with the few measured data points.

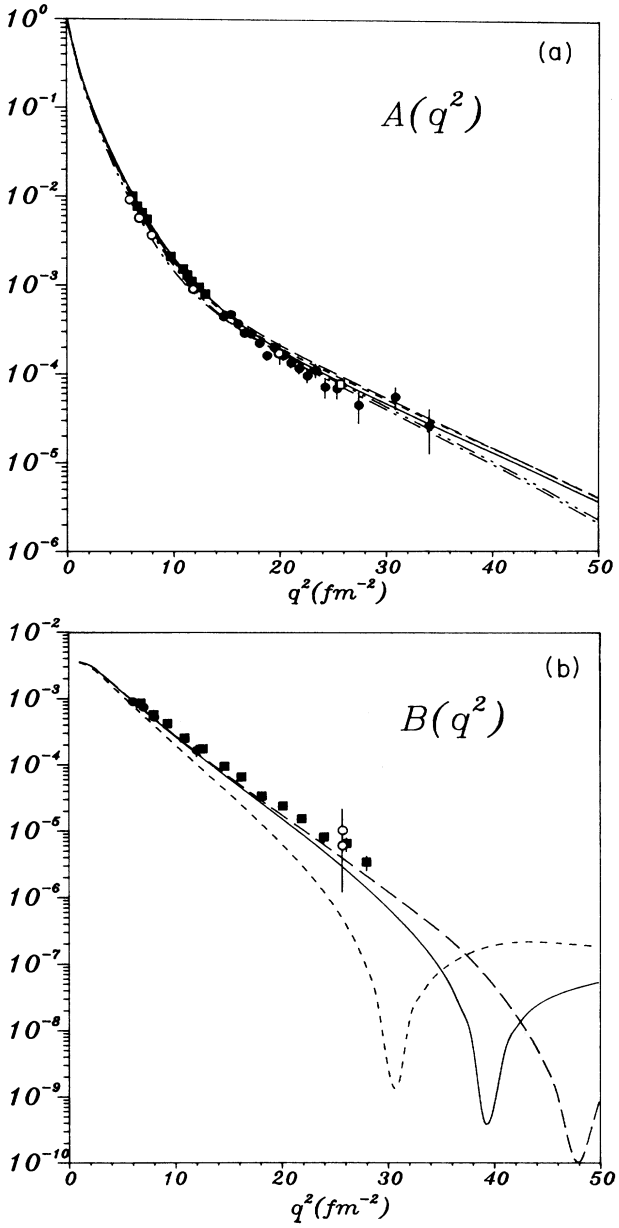

FIG. 7. Deuteron structure functions $A(q^2)$ and $B(q^2)$. (a) Dashed line denotes our model with $b=1$ fm; solid line, our model with $b=1$ fm including $F_{6q}(q^2)$; long-dashed—two-dotted line, our model with $b=1.2$ fm; long-dashed—dotted line, our model with $b=1.2$ fm including $F_{6q}(q^2)$; long dashed line, RSC. Experiments, Ref. 31. (b) Dashed line denotes our model with $b=1.2$ fm; solid line, our model with $b=1$ fm; long-dashed line, RSC. Experiments, Refs. 31 and 32.

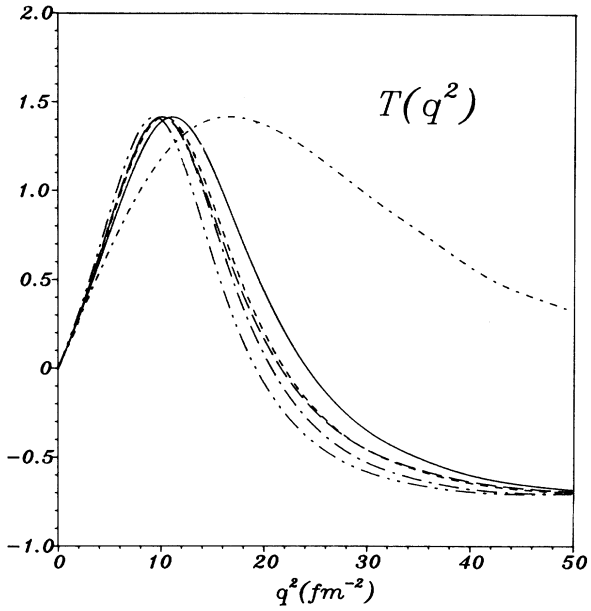

FIG. 8. Deuteron polarization tensor $T(q^2)$ of Eq. (28). Dashed line denotes our model with $b=1$ fm; solid line, our model with $b=1$ fm including $F_{6q}(q^2)$; long-dashed—two-dotted line, our model with $b=1.2$ fm; long-dashed—dotted line, our model with $b=1.2$ fm including $F_{6q}(q^2)$; long dashed line, RSC; dash dotted line, RSC including $F_{6q}(q^2)$ using parameters of Ref. 30 (in contrast to Ref. 30, we also included MEC's as explained in the text).

Note that for the polarizations there is also no sizable difference between various potentials in the momentum range measured so far, in contrast to the magnetic form factor. To conclude this section we would highly recommend studying deuteron observables from quark-model motivated potentials, since we found some sensitivity to the core parameters in elastic electron deuteron scattering.

VI. SUMMARY AND CONCLUSION

We have constructed and discussed a NN potential that is reasonably consistent with the internal quark structure of the nucleon both in short range and medium-long range parts, which is in sharp contrast to conventional NN potentials.[4] The short range part is phenomenological and the medium/long range parts are of mesonic origin but contain only two adjusted parameters in the TPE range (three if one chooses to fit m_σ also).

The mesons are effective particles but handled as point-like in the sense of elementary particles. Quark-meson coupling constants and regularizations of the meson-

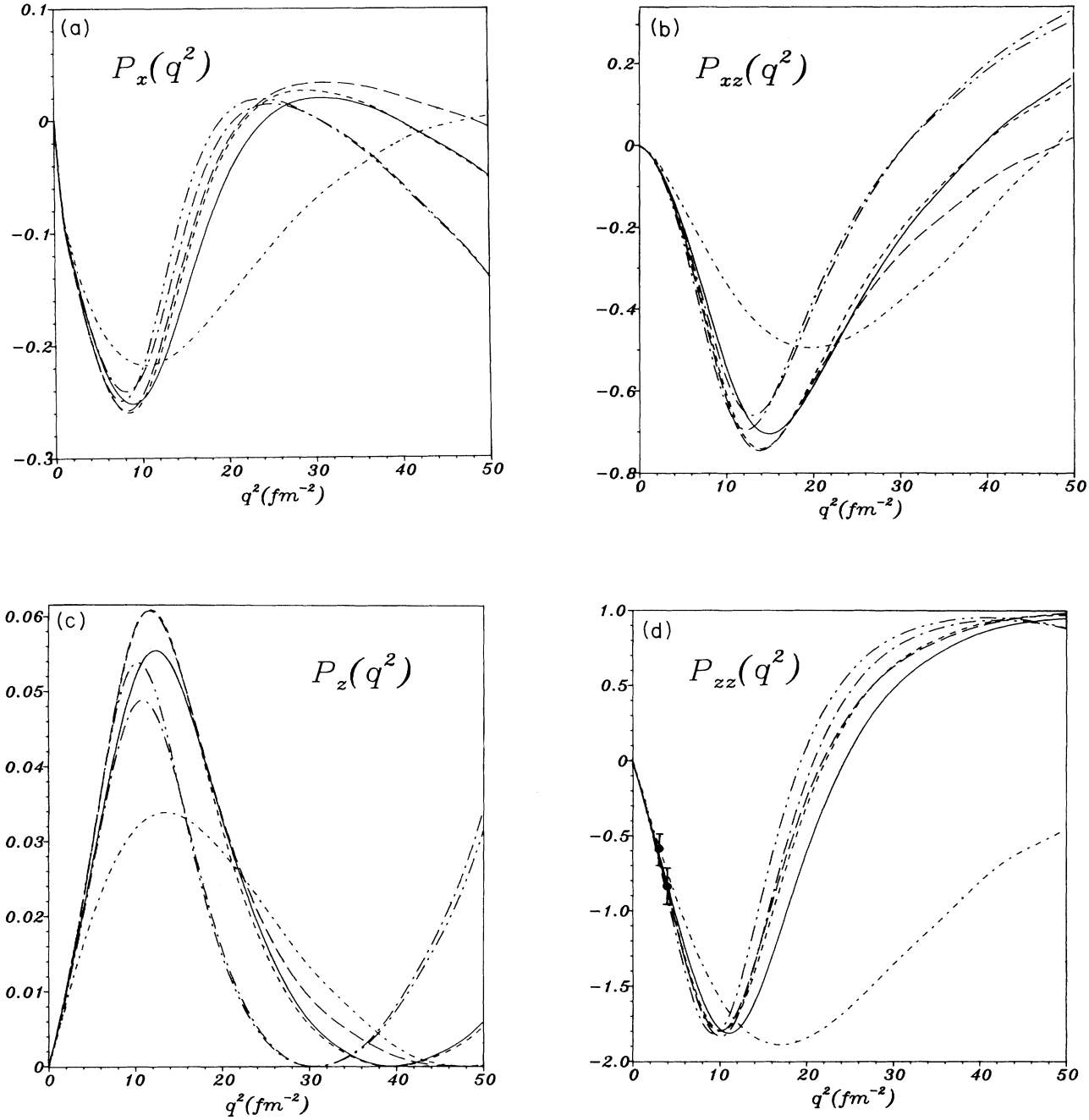

FIG. 9. Deuteron polarization observables P_x, P_z, $P_{xz'}$, P_{zz}, and $\theta=70°$. For curves, see caption of Fig. 8. Experiments are from Ref. 33.

baryon vertices are provided by the quark confinement model, taken to be a quasirelativistic constituent quark model (CQM). This quark model has been applied with considerable success to calculate many observables of the nucleon.[13–17]

The NN potential is extended inside of the NN overlap region by an optical potential description of the six-quark core. This phenomenology gives an appropriate handling of the six-quark system in view of the continued absence of a complete six-quark Hamiltonian. It is this lack of knowledge of quark dynamics which leads to 15 additional parameters (over and above the two parameters in the meson potential to fit the TPE sector properly), to be extracted from the phase shift analysis. There is some hope to eliminate some of these parameters, if a reasonable model of the six-quark system is found.

In this framework we have investigated the dependence of NN phase shifts and deuteron observables on the radius

of the six-quark core. For $1 \leq b \leq 1.2$ fm our model gives equally good descriptions of the NN scattering data below the pion production threshold and the static properties of the deuteron. However, the magnetic form factor $B(q^2)$ of the deuteron for $q^2 \geq 20$ fm^{-2} restricts the six-quark core radius further below $b \leq 1$ fm.

We conclude that, since we have extracted six-quark parameters from NN phase shifts, it is now possible to apply such quark core potential to other processes, e.g., electromagnetic form factors of triton-^{3}He systems or nuclear matter calculations, which may be useful to refine our knowledge of the core parametrization further. The main problem to be solved consists in finding the proper dynamics of the six-quark core to evaluate the short range contributions.

ACKNOWLEDGMENTS

This work was supported in part by the Deutsche Forschungsgemeinschaft (Sonderforschungsbereich 201) and in part by the U.S. National Science Foundation.

*Present address: Institute for Nuclear Theory, Department of Physics, FM-15, University of Washington, Seattle, WA 98195.

[1]K. Huang, *Quarks, Leptons and Gauge Fields* (World-Scientific, Singapore, 1982), and references therein.

[2]F. Close, *An Introduction to Quarks and Partons* (Academic, London, 1979), and references therein.

[3]For a review of the vast literature, see A. W. Thomas, Adv. Nucl. Phys. **13**, 1 (1983).

[4]See, e.g., *Proceedings of the Second International Conference on Nucleon-Nucleon Interactions,* AIP Conf. Proc. No. 41, edited by D. Measday, H. Fearing, and A. Strathdee (AIP, New York, 1978); M. Lacombe *et al.*, Phys. Rev. C **21**, 861 (1980); K. Erkelenz, Phys. Rep. **13C**, 191 (1974); K. Holinde, *ibid.* **68C**, 121 (1981); G. E. Brown and A. D. Jackson, *The Nucleon-Nucleon Interaction* (North-Holland, Amsterdam, 1976).

[5]See, e.g., H. Arenhövel and J. M. Laget, in *New Vistas in Electronuclear Physics,* NATO Advanced Study Series (Plenum, New York, 1985).

[6]T. E. O. Ericson and M. Rosa-Clot, Nucl. Phys. **A405**, 497 (1983).

[7]G. 't Hooft, Nucl. Phys. **B72**, 461 (1974); E. Witten, *ibid.* **B160**, 57 (1979).

[8]See, e.g., in *Proceedings of the Lewes Workshop on Solitons in Nuclear and Particle Physics,* edited by A. Chodos, E. Hadjimichael, and C. Tze (World-Scientific, Singapore, 1984).

[9]Y. Nambu and G. Jona-Lasinio, Phys. Rev. **122**, 345 (1961); T. Eguchi, *ibid.* D **10**, 4257 (1974).

[10]D. Ebert and M. K. Volkov, Z. Phys. C **16**, 205 (1983).

[11]J. J. Sakurai, *Currents and Mesons* (University of Chicago, Chicago, 1969).

[12]M. Bando *et al.*, Phys. Rev. Lett. **54**, 1215 (1985); H. Stremnitzer, University of Maryland Report No. 86-20, 1985.

[13]M. Beyer and H. J. Weber, Phys. Lett. **146B**, 383 (1984); M. Bozoian and H. J. Weber, Phys. Rev. C **28**, 811 (1983).

[14]J. Cohen and H. J. Weber, Phys. Lett. **165B**, 229 (1985).

[15]M. Beyer and S. K. Singh, Phys. Lett. **160B**, 26 (1985).

[16]M. Beyer and S. K. Singh, Z. Phys. C **31**, 421 (1986).

[17]H. J. Weber and M. Weyrauch, Phys. Rev. C **32**, 1342 (1985).

[18]E. V. Shuryak, Nucl. Phys. **B203**, 93 (1982); **B203**, 116 (1982); **B203**, 140 (1982).

[19]M. A. Shifman, A. I. Vainstein, and V. I. Zakharov, Nucl. Phys. **B147**, 385 (1979); **B147**, 448 (1979); **B147**, 519 (1979).

[20]Yu. A. Simonov, Phys. Lett. **107B**, 1 (1981); S. M. Dorkin, V. K. Lukyanov, and A. I. Titov, Z. Phys. A **316**, 331 (1984).

[21]B. L. G. Bakker, I. L. Grach, and I. M. Narodetskij, Nucl. Phys. **A424**, 563 (1984).

[22]Note that in V. S. Bhasin and V. K. Gupta, Phys. Rev. C **32**, 1187 (1985), the sign of the pole term in their Eq. (12) is incorrect. As a consequence the fitted values of E_0 are unusually low.

[23]B. L. G. Bakker *et al.*, Phys. Rev. C **25**, 1134 (1982).

[24]R. Arndt *et al.*, Phys. Rev. D **28**, 97 (1983).

[25]E. Lomon, Phys. Rev. D **26**, 576 (1982); in *Proceedings of the Tenth International Conference on Particles and Nuclei,* edited by B. Povh and G. zu Putlitz (North-Holland, Amsterdam, 1984), p. 139.

[26]L. S. Kisslinger, Phys. Lett. **112B**, 307 (1982); E. M. Henley, L. S. Kisslinger, and G. A. Miller, Phys. Rev. C **27**, 1602 (1983).

[27]T.-S. Cheng and L. S. Kisslinger, Carnegie-Mellon University report, 1986.

[28]Yu. S. Kalashnikova, I. M. Narodetskij, and A. I. Veselov, Z. Phys. A **323**, 205 (1986).

[29]M. Beyer, D. Drechsel, and M. Giannini, Phys. Lett. **122B**, 1 (1983).

[30]V. V. Burov, S. M. Dorkin, and V. N. Dostovalov, Z. Phys. A **315**, 205 (1984).

[31]C. D. Buchanan and M. R. Yearin, Phys. Rev. Lett. **15**, 303 (1965); J. E. Elias *et al.*, Phys. Rev. **177**, 2075 (1969); S. Galster *et al.*, Nucl. Phys. **B32**, 221 (1971); F. Martin *et al.*, Phys. Rev. Lett. **38**, 1320 (1977).

[32]S. Auffret *et al.*, Phys. Rev. Lett. **54**, 649 (1985).

[33]M. E. Schulze *et al.*, Phys. Rev. Lett. **52**, 597 (1984).